ARTICLE - Non-Hodgkin Lymphoma

Prognostic relevance of tumor-infiltrating CD4$^+$ cells and total metabolic tumor volume-based risk stratification in diffuse large B-cell lymphoma

Daisuke Ikeda,[1] Mitsuaki Oura,[1] Atsushi Uehara,[1] Rikako Tabata,[1] Kentaro Narita,[1] Masami Takeuchi,[1] Youichi Machida[2] and Kosei Matsue[1]

[1]Division of Hematology/Oncology, Department of Medicine, Kameda Medical Center and [2]Department of Radiology, Kameda Medical Center, Chiba, Japan

Correspondence: D. Ikeda
dskikd.2409@gmail.com

Received: January 10, 2024.
Accepted: March 28, 2024.
Early view: April 4, 2024.

https://doi.org/10.3324/haematol.2024.285038

Supplementary methods

Patient cohort and study design

We conducted a retrospective analysis of newly diagnosed patients with histologically confirmed DLBCL who were treated with rituximab (RTX) plus cyclophosphamide (CY), doxorubicin (DXR), vincristine (VCR), and prednisone (PSL) (R-CHOP) or R-CHOP-like chemotherapy at Kameda Medical Center between 2006 and 2020. The R-CHOP-like regimen was categorized as either a more intensive chemotherapy, defined as RTX combined with etoposide, PSL, VCR, CY, and DXR (R-EPOCH), or hyperfractionated CY, VCR, DXR and dexamethasone (R-HyperCVAD), or a less intensive treatment such as R-CHOP without DXR (R-CVP) or without VCR (R-CHP). The primary exclusion criteria were the absence of pre-treatment PET/CT with FDG-avid lesions and the insufficient flow cytometric (FCM) data from biopsied lymphoma lesions. Patients with high-grade B-cell lymphoma harbouring concurrent rearrangements of *MYC*, *BCL2*, or *BCL6* were also excluded. Patients with untreated histologically transformed follicular lymphoma (tFL) and Epstein-Barr virus (EBV)-positive DLBCL were not excluded. No cases of T-cell/histiocyte-rich large B-cell lymphoma pathologically confirmed were observed in the entire cohort. The DLBCL cell of origin was determined using immunohistochemistry (IHC) according to the Hans algorithm.[1] The pathological diagnosis was made by expert haematopathologists according to the 2016 revision of the World Health Organization classification.[2] The response to first-line treatment was evaluated at the end of induction based on the Lugano 2014 criteria.[3] The flow diagram of patient enrolment is shown in Supplementary Figure 1. Due to the large number of patients excluded because of unavailable or inappropriate FCM data, baseline clinical characteristics were compared between those with and without FCM data (Supplementary Table 1). All clinical factors were not significantly different, except for the older age in patients excluded from the analysis (median 74 vs. 71 years, P=0.006). Unexpectedly, patients who were not able to obtain sufficient samples for FCM were significantly more likely to have biopsies from extranodal lesions (54.7% vs. 15.8%, P <0.001), including the gastrointestinal (GI) tract. Concerning clinical outcomes, the 171 included and 347 excluded patients showed comparable 3-year progression free survival (PFS) (58.3% 95% confidence interval [CI]: 51.3%-66.3% vs. 61.4% 95% CI: 56.2%-67.0%, P = 0.35) and OS rates (72.6% 95% CI: 66.2%-79.7% vs. 68.5% 95% CI 63.5%-73.9, P = 0.77, respectively). The present study was conducted in accordance with the Declaration of Helsinki and was approved by our institutional review board (approval number: 22-095). The dataset was locked on July 31, 2023.

PET-CT imaging procedures

All PET/CT images were acquired using PET/CT scanners (Discovery ST Elite Performance, GE Medical

Systems, Milwaukee, WI, USA [January 2011 to June 2017]; Discovery IQ ODYSSEY 5R, GE Medical Systems, Milwaukee, WI, USA [June 2017 to July 2021]) according to our institution's standardized protocol.[4] Initially, patients were prepared by fasting for at least six hours, discontinuing any anti-diabetic therapies, and ensuring that serum glucose levels remained within 200 mg/dL. Subsequently, patients received an intravenous injection of a standard dose of 4.3 MBq/kg ^{18}FDG (maximum 350 MBq). Between sixty to seventy-five minutes post-FDG injection, a low-dose CT scan (120kV and 150mA) was obtained and combined with a PET scan, imaging from the skull to the midthigh level. The CT acquisition was performed with a tube rotation of 0.5 seconds, section thickness of 3.26 mm, and a pitch of 1.375:1. The matrix and voxel sizes of the acquired images were 128 × 128 and 3.75 × 3.75 × 3.75 mm for Discovery ST Elite Performance and 192 × 192 and 3.26 × 3.26 × 3.26 mm for Discovery IQ ODYSSEY 5R. Once reconstructed, the PET/CT images were evaluated by a well-trained nuclear medicine physician (YM), who was blinded to the clinical data.

Measurement of PET/CT-derived parameters

The standardized uptake value (SUV) was calculated using the following formula: tissue radioactivity concentration (Bq/mL) divided by the injected dose (Bq) per body weight (g). Total metabolic tumour volume (TMTV) was defined as the sum of the volume of visually identified lymphoma lesions with an SUV of ≥ 4 as the absolute threshold.[5] Total lesion glycolysis (TLG) was calculated by multiplying TMTV by mean SUV. For tumour delineation and calculation of radiomic parameters, a semi-automatic computer-aided analysis of PET/CT images was conducted using the open-source software Metavol (Hokkaido University, Sapporo, Japan).[6] The Metavol software automatically highlights all voxels with an SUV≥4.0 from the entire image. We then manually excluded physiological uptakes, including those in the brain, heart, and urinary tract, as well as any apparent inflammatory accumulations. As per a previous proposal,[7] increased ^{18}FDG uptake in the spleen was considered lymphoma involvement only if there were focal areas with ^{18}FDG uptake 1.5 times greater than that in the liver, while bone marrow involvement was included in volume measurements if focal lesions were present, irrespective of the intensity of ^{18}FDG uptake.

Quantification of intratumoural cell populations

Samples obtained from lymph nodes or extranodal lesions were processed immediately after the biopsy. After the mechanical dissociation, the tissues were filtered through a 40-µm nylon mesh and then centrifuged at 500g for 15 minutes at room temperature, after which the supernatant was carefully decanted.[8] The cell pellet was then washed with phosphate-buffered saline. Subsequently, the cells were stained with a panel of antibodies including CD45-KrO, CD19-APC, CD3-FITC, CD4-FITC, CD8-PE, and CD56-

PE (if available). Within the acquired mononuclear cells, the proportions of CD19+, CD3+, CD4+, CD8+, and CD56+ cells were quantified after gating based on the characteristic forward and side scatter patterns and CD45 positivity specific to lymphocytes. While the tissue sampling manner was not strictly limited to an excisional biopsy, a minimum of 10000 mononuclear cells per sample was required, based on a previous study.[9] Data were acquired on a Navios flow cytometer using the Kaluza software (Beckman Coulter, CA, USA).

Statistical analysis

Statistical analyses were performed with R version 4.1.1 (R Foundation, Vienna, Austria). Continuous variables were analysed using the Mann–Whitney U test, while categorical variables were compared using the Fisher's exact test. Pearson correlation analysis was employed to examine the relationships between radiomic features and cellular content within tumours. To maximize predictive power, optimal cut-off values were determined using receiver operating characteristic (ROC) curves for 3-year PFS and 3-year OS. The DeLong's test was used to compare the areas under the curve from two correlated ROCs. The PFS and OS were estimated using the Kaplan–Meier methods and compared with the log-rank test. Univariate and multivariate analyses were conducted using Cox proportional hazards models to assess the factors affecting PFS and OS. Statistical significance was defined as a two-sided P-value of <0.05.

References (supplementary methods)

1. Hans CP, Weisenburger DD, Greiner TC, et al. Confirmation of the molecular classification of diffuse large B-cell lymphoma by immunohistochemistry using a tissue microarray. Blood. 2004;103(1):275-82.

2. Swerdlow SH, Campo E, Pileri SA, et al. The 2016 revision of the World Health Organization classification of lymphoid neoplasms. Blood. 2016;127(20):2375-90.

3. Cheson BD, Fisher RI, Barrington SF, et al. Recommendations for initial evaluation, staging, and response assessment of Hodgkin and non-Hodgkin lymphoma: the Lugano classification. J Clin Oncol. 2014;32(27):3059-68.

4. Terao T, Machida Y, Hirata K, et al. Prognostic Impact of Metabolic Heterogeneity in Patients With Newly Diagnosed Multiple Myeloma Using 18F-FDG PET/CT. Clin Nucl Med. 2021;46(10):790-6.

5. Kurtz DM, Green MR, Bratman SV, et al. Noninvasive monitoring of diffuse large B-cell lymphoma by immunoglobulin high-throughput sequencing. Blood. 2015;125(24):3679-87.

6. Hirata K, Kobayashi K, Wong KP, et al. A semi-automated technique determining the liver standardized uptake value reference for tumor delineation in FDG PET-CT. PLoS One. 2014;9(8):e105682.

7. Barrington SF, Meignan M. Time to Prepare for Risk Adaptation in Lymphoma by Standardizing Measurement of Metabolic Tumor Burden. J Nucl Med. 2019;60(8):1096-102.

8. Witzig TE, Banks PM, Stenson MJ, et al. Rapid immunotyping of B-cell non-Hodgkin's lymphomas by flow cytometry. A comparison with the standard frozen-section method. Am J Clin Pathol. 1990;94(3):280-6.

9. Keane C, Gill D, Vari F, Cross D, Griffiths L, Gandhi M. CD4(+) tumor infiltrating lymphocytes are prognostic and independent of R-IPI in patients with DLBCL receiving R-CHOP chemo-immunotherapy. Am J Hematol. 2013;88(4):273-6.

Supplementary Table 1. Comparison of baseline characteristics between patients with or without sufficient FCM data

	Patients without sufficient FCM data (n=258 [60.1%])	Patients included for analysis (n=171 [39.9%])	P-value
Age, year, median (IQR)	74 (66-80)	71 (61-79)	0.006
Age >60, n (%)	227 (88.0)	130 (76.0)	0.002
Female, n (%)	119 (46.1)	80 (46.7)	0.972
ECOGPS ≧2, n (%)	78 (30.2)	37 (21.4)	0.063
LDH >UNL, n (%)	172 (66.7)	115 (67.8)	0.983
Ann Arbor stage ≧3, n (%)	154 (59.7)	101 (59.1)	0.977
Number of EN lesions ≧2, n (%)	80 (31.0)	38 (22.2)	0.059
IPI, n (%)			
0-2	115 (44.6)	89 (52.0)	-
3-5	143 (55.4)	82 (48.0)	0.156
Disease type, n (%)			
DLBCL, NOS	242 (93.8)	156 (91.2)	0.414
t-FL	12 (4.7)	8 (4.7)	1
EBV-positive DLBCL	4 (1.6)	7 (4.1)	0.187
COO according to Hans algorithm, n (%)			
GCB type	81 (31.4)	48 (28.1)	0.53
non-GCB type	118 (45.7)	89 (52.0)	0.237
Missing	59 (22.9)	34 (19.9)	0.539
PET/CT parameters, median (IQR)			
SUVmax	19.6 (14.4-26.5)	20.8 (14.9-26.9)	0.573
TMTV (mL)	176.2 (51.5-530.2)	177.8 (47-560)	0.961
TLG	1418.3 (384.8-4637.5)	1683.4 (352-5557.4)	0.832

Biopsied lesion, n (%)			
LN	117 (45.3)	144 (84.2)	<0.001
EN lesion	141 (54.7)	27 (15.8)	<0.001
GI tracts	58 (22.5)	3 (1.8)	<0.001
BM	14 (5.4)	0 (0)	0.005
Other lesions	69 (26.7)	24 (14.0)	0.003
Induction regimen, n (%)			
R-CHOP	220 (85.3)	149 (87.1)	0.687
More intensive chemotherapy	20 (7.8)	13 (7.6)	1
Less intensive chemotherapy	18 (7.0)	9 (5.3)	0.608
CR achievement at end of induction, n (%)	193 (74.8)	139 (81.3)	0.146

Abbreviations: TI, tumour-infiltrating; IQR, interquartile range; ECOGPS, European Cooperative Oncology Group Performance Status; LDH, lactate dehydrogenase; UNL, upper normal limit; EN, extranodal; IPI, International Prognostic Index; DLBCL, NOS, diffuse large B-cell lymphoma, not otherwise specified; t-FL, DLBCL transformed from follicular lymphoma; EBV, Epstein-Barr virus; COO, cell of origin; GCB, germinal center B-cell; SUV, standard uptake value; TMTV, total metabolic tumour volume; TLG, total lesion glycolysis; LN, lymph node; EN, extranodal; GI, gastrointestinal; BM, bone marrow; R-CHOP, rituximab combined with cyclophosphamide, doxorubicin, vincristine, and prednisone; CR, complete remission.

Supplementary Figure 1. Flow diagram of patient enrolment for analysis.

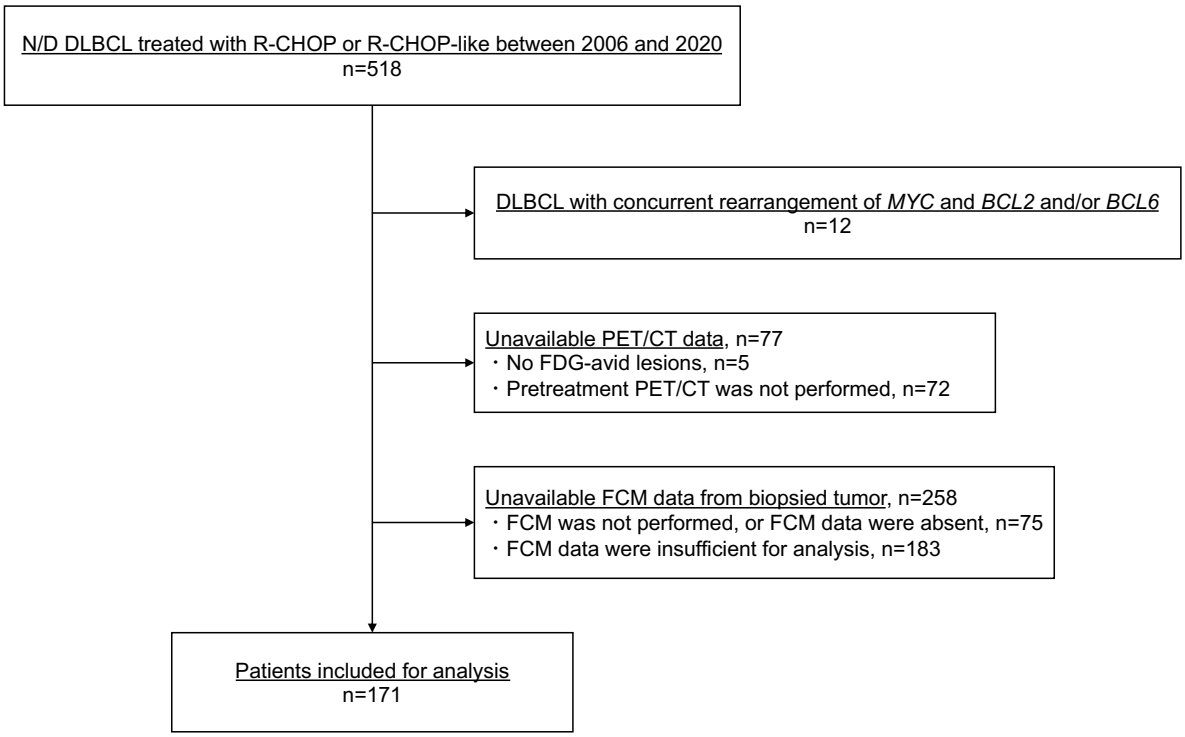

Abbreviations: N/D, newly diagnosed; DLBCL, diffuse large B-cell lymphoma; FDG, Fluorine-18 fluorodeoxyglucose; PET/CT, positron emission tomography/computed tomography; FCM, flow cytometry.

Supplementary Figure 2. ROC analysis to determine optimal cut-offs for predicting 3-year PFS and OS.

A) ROC for intratumoural lymphocyte subsets and B) ROC for radiomic parameters.

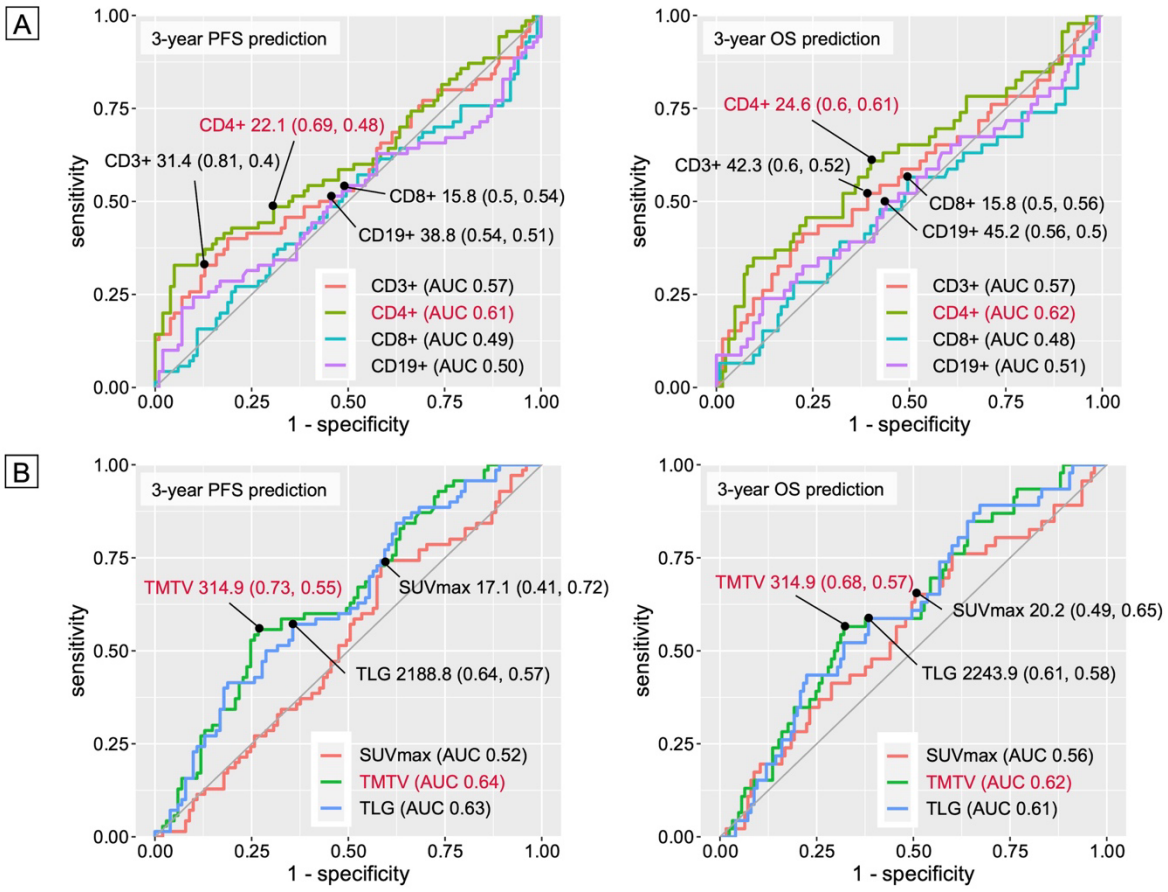

Abbreviations: PFS, progression-free survival; OS, overall survival; AUC, area under the curve; TMTV, total metabolic tumour volume; TLG, total lesion glycolysis.

Supplementary Figure 3. Comparison of tumour-infiltrating cell proportions between EBV-positive and EBV-negative DLBCL patients. A) CD19+ cells, B) CD3+ cells, C) CD4+ cells, and D) CD8+ cells.

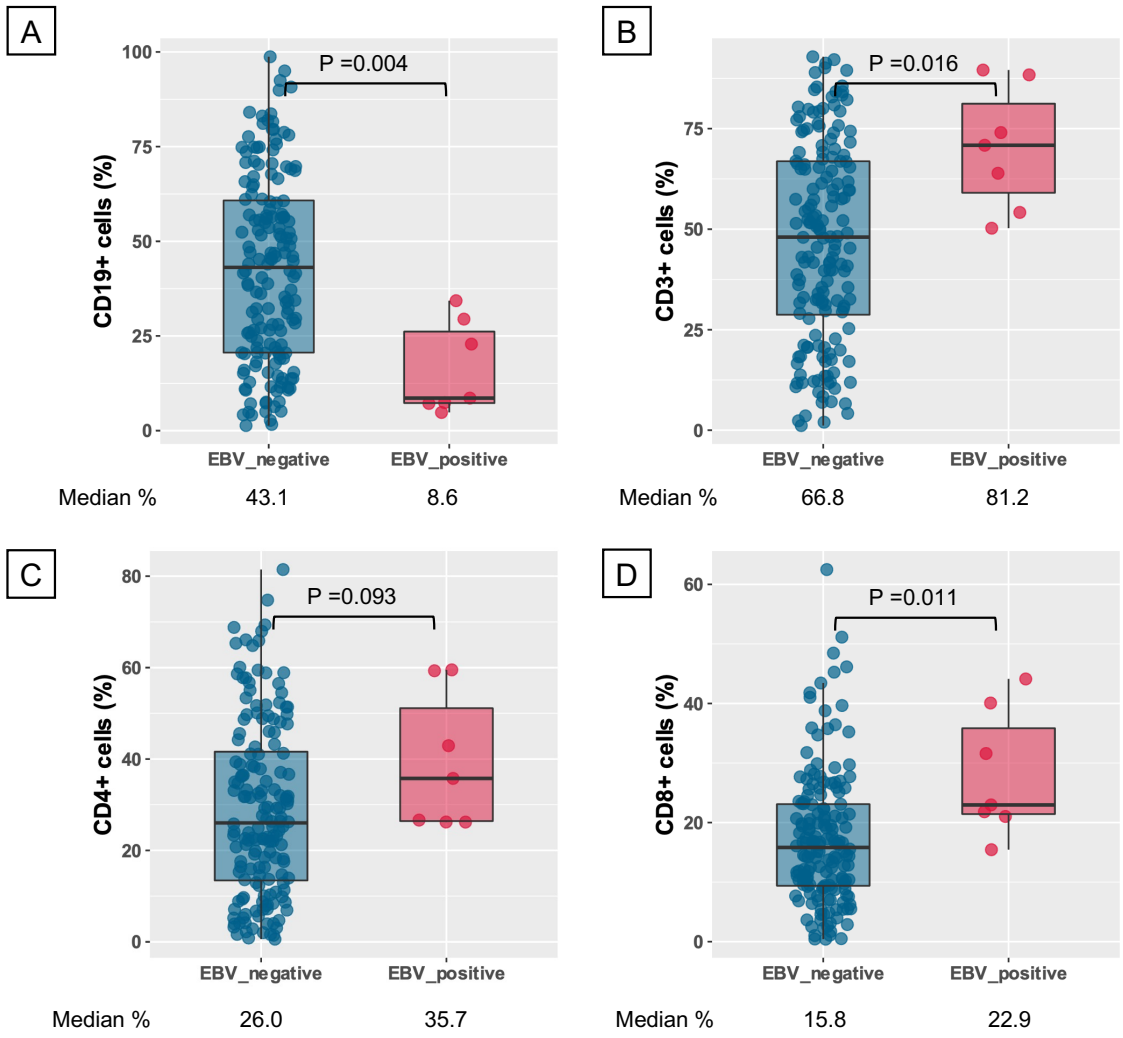

Abbreviations: EBV, Epstein-Barr virus; DLBCL, diffuse large B-cell lymphoma.

Supplementary Figure 4. Prognostic relevance of tumour-infiltrating CD4+ cells in biopsied extranodal lesions. A) Pie chart showing the distribution of biopsied organs. B) Comparison of intratumoural lymphocyte proportions between lymph nodes and extranodal lesions. C) Kaplan-Meier estimates of OS and D) PFS based on the CD4+ cell burden within extranodal lesions.

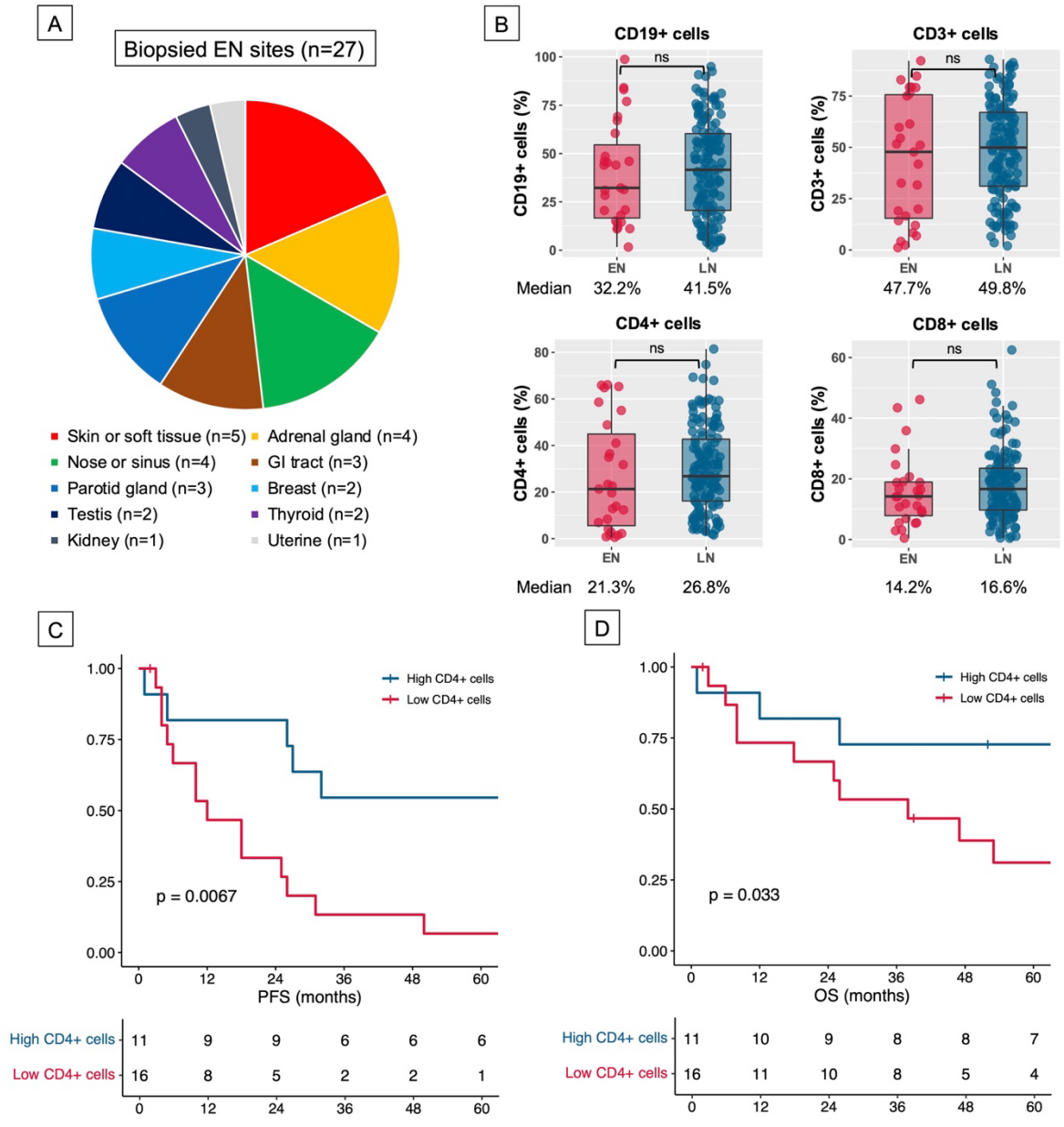

Abbreviations: EN, extranodal; PFS, progression-free survival; OS, overall survival.